On Texture Analysis: Local Energy Transforms versus Quadrature Filters

Til Aach and André Kaup and Rudolf Mester

in: Signal Processing. See also BibTeX entry below.

BibTeX:

```
@article{AAC95a,
author = {Til Aach and Andr\'e Kaup and Rudolf Mester},
title = {On Texture Analysis: Local Energy Transforms
   versus Quadrature Filters},
journal = {Signal Processing},
        publisher       = {Elsevier},
volume = {45},
number = {2},
year = {1995},
pages = {173--181}}
```

SIGNAL PROCESSING

ELSEVIER Signal Processing 45 (1995) 173-181

On texture analysis: Local energy transforms versus quadrature filters

Til Aach[a,*], André Kaup[a], Rudolf Mester[b]

[a] *Institute for Communication Engineering, Aachen University of Technology (RWTH), D-52056 Aachen, Germany*
[b] *Robert Bosch GmbH, Research Institute Hildesheim, D-31132 Hildesheim, Germany*

Received 1 July 1993; revised 12 August 1994 and 26 March 1995

Abstract

The well-known method proposed by Laws for texture analysis first subjects the texture to a filter bank, followed by the computation of energy measures, e.g. through local variance estimation. As shown by Unser in 1986, the filter bank application is equivalent to a linear transformation of the grey values of neighbouring pixels. In this contribution, we derive a further linear relationship between the local variances of the filter outputs and the autocorrelation function of the texture process. Furthermore, we examine how the filter bank approach is related to another method based on multifiltering, namely that one using quadrature filter pairs, by means of which the amplitude envelopes of the filtered texture signal can be obtained. It is shown that the texture energy method can be understood as the equivalent of an envelope detector receiver commonly used in AM communication techniques. Feature images provided by the texture energy method are compared with their counterparts resulting from the quadrature filter approach, and criteria helping to decide when to use which one of the methods are given.

Zusammenfassung

Eine bekannte, von Laws vorgeschlagene Methode zur Texturanalyse besteht in der Filterung der Textursignale mit einer Filterbank, an deren Ausgängen dann Maße für die Leistung der gefilterten Textur berechnet werden, z.B. durch lokale Estimation der Varianz. Wie 1986 von Unser gezeigt wurde, entspricht die Filterung der Texturen mit der Filterbank einer linearen Transformation der Grauwerte benachbarter Pixel. In diesem Beitrag wird eine weitere lineare Beziehung zwischen den lokal geschätzten Varianzen der Filterausgangssignale und der Autokorrelationsfunktion des Texturprozesses abgeleitet. Weiter wird untersucht, in welchem Zusammenhang dieser Filterbank-Ansatz mit derjenigen Multi-Filter-Methode steht, welche durch Quadratur-Filterung die Hüllkurven des bandpaßgefilterten Textursignales erzeugt. Es wird gezeigt, daß die Texturenergie-Methode als Äquivalent eines Hüllkurvenempfängers aufgefaßt werden kann, der in der AM-Kommunikation gewöhnlich eingesetzt wird. Durch die Texturenergie-Methode erzeugte Merkmalsbilder werden mit ihren aus dem Quadraturfilter-Ansatz resultierenden Gegenstücken verglichen, und Kriterien zur Auswahl des geeigneten Texturanalyseverfahrens gegeben.

Résumé

La methode bien connue proposée par Laws pour l'analyse de texture soumet d'abord la texture à un banc de filtres, suivi par le calcul de mesures de l'énergie, i.e. par estimation de variances locales. Comme Unser l'a montré en 1986,

* Corresponding author. Present address: Philips GmbH Research Labs., Weißhausstr. 2, D-52066 Aachen, Germany.

0165-1684/95/$9.50
SSDI 0165-1684(95)00049-6

l'application des bancs de filtres est équivalente à une transformation linéaire des valeurs de gris de pixels voisins. Dans cette contribution, nous dérivons une relation linéaire supplementaire entre les variances locales des sorties de filtre et la fonction d'autocorrelation du processus de texture. De plus, nous examinons de quelle manière l'approche par bancs de filtres est apparentée à une autre méthode basée sur le filtrage multiple, en d'autres termes celle utilisant des paires de filtres en quadrature, à l'aide desquels l'enveloppe de l'amplitude du signal de texture filtré peut être obtenue. On montre que la méthode d'énergie de texture peut être comprise comme l'équivalent d'un récepteur détecteur d'enveloppe communènement utilisé dans les techniques de communication AM. Les images de caractéristiques fournies par la methode d'énergie de texture sont comparées à leurs contreparties obtenues par l'approche utilisant les filtres en quadrature, et des critères permettant de décider quand utiliser l'une ou l'autre méthode sont donnés.

Keywords: Texture analysis; Texture energy measures; Quadrature filter pairs; Gabor filters; Envelope demodulation; AM communications

1. Introduction

The characterization of textured areas in natural images is a fundamental task in a variety of image processing problems, such as classification and recognition, or segmentation. In this context, the term *texture* generally refers to some property attributed to sets of adjacent pixels, or neighbourhoods. Regarding the observed grey levels of a neighbourhood as realization of a random vector, statistical approaches to texture analysis focus on revealing features of the joint probability density of the components of the random vector [10]. This can for instance be done by the computation of univariate or multivariate statistics, like in the co-occurrence matrix approach [26]. A computationally much more efficient alternative is based on applying a filter bank to the texture signal [3, 6, 11, 20, 24, 25]. The well-known texture energy measures [14], for instance, are computed by first convolving the given texture signal $s(k, l)$ with a set of small FIR filter masks $h_i(k, l)$, $i = 1, \dots, N$, resulting in a set of so-called feature planes $g_i(k, l)$. Assuming the texture signal as stationary, energy measures like estimates of the feature plane variances σ_i^2 are obtained through the estimation of local univariate statistics by spatial averaging inside each feature plane. Whereas Laws' approach [14] is empirical and rather ad hoc, Unser in a later contribution [23] gives a detailed justification of texture measurements by filter bank analysis. He points out that the outputs $g_i(k, l)$ of the filter bank are a linear transform of the local neighbourhood vector $\boldsymbol{s}_{kl}$ according to

$$\boldsymbol{g}_{kl} = \boldsymbol{H} \cdot \boldsymbol{s}_{kl} \quad \text{with } \boldsymbol{H} = \begin{bmatrix} \boldsymbol{h}_1^{\mathrm{T}} \\ \vdots \\ \boldsymbol{h}_N^{\mathrm{T}} \end{bmatrix}, \tag{1}$$

where $\boldsymbol{g}_{kl}$ is a column vector obtained by lexicographically ordering the N filter outputs $g_i(k, l)$. The neighbourhood vector $\boldsymbol{s}_{kl}$ is similarly formed by ordering the grey values $s(m, n)$ lying inside the support area of the filter masks centred at (k, l). Commonly used are filters of square support, with the number of filters equal to the number of coefficients of each filter, i.e. when denoting the filter support area by $M \times M$, we have $N = M^2$. Finally, the row vectors $\boldsymbol{h}_i^{\mathrm{T}}$ result from ordering the coefficients of the filter masks $h_i(m, n)$.[1] One advantage of the filter bank approach is that structural information – otherwise to be evaluated by the computationally demanding estimation of multivariate statistics of $s(k, l)$ – is now reflected in (estimates of) univariate moments of the random variables in the feature planes. The obvious reason for this is that each filter combines the grey levels $s(m, n)$ of the pixels covered by its support area to an output value. The mentioned channel variances σ_i^2, for

[1] Using a number of filters which is identical to the number of filter coefficients and hence to the dimension N of the neighbourhood vector means that the matrix $\boldsymbol{H}$ is quadratic and invertible, provided the filters are linearly independent.

instance, can be computed from the covariance matrix C_s of s_{kl} by

$$\sigma_i^2 = h_i^{\mathrm{T}} \cdot C_s \cdot h_i. \tag{2}$$

They thus depend on the covariances of $s(k, l)$ [23], and hence also on the probability density $p(s_{kl})$ which fully describes the neighbourhood random vector.

2. Texture energy transforms

So far, we have recalled that the linear relationship (1) exists between the texture $s(k, l)$ and the feature planes $g_i(k, l)$, with the connection between the channel variances σ_i^2 and the covariances of $s(k, l)$ being made by (2). For *stationary* signals, however, the quadratic form (2) can be simplified to a linear relationship, too, by exploiting the Toeplitz structure of C_s. In this section, however, we take a different approach which shows that the set of (theoretical) channel variances is a linear transform of the autocorrelation function of the texture process within a certain window. Following [2], we will see that the coefficients of the transformation matrix are determined by the aperiodic autocorrelation functions of the convolution masks $h_i(k, l)$.

Without loss of generality, we assume that $s(k, l)$ is a zero-mean process. With $r_g^i(k, l)$ denoting the autocorrelation function (ACF) of the ith feature plane $g_i(k, l)$, the variance σ_i^2 is given by

$$\sigma_i^2 = r_g^i(0,0), \quad i = 1, \ldots, N. \tag{3}$$

As $g_i(k, l)$ is the result of convolving $s(k, l)$ with the filter $h_i(k, l)$, the ACF $r_g^i(k, l)$ can be determined from the ACF $r_s(k, l)$ of the texture process and the (aperiodic, [18, Chapter 8.4]) autocorrelation function $r_h^i(k, l)$ of the filter $h_i(k, l)$ through the Wiener–Lee theorem [15], which holds for stationary signals:

$$r_g^i(k, l) = r_s(k, l) * r_h^i(k, l)$$
$$= \sum_{m,n} r_s(m, n) \cdot r_h^i(k - m, l - n), \tag{4}$$

where the asterisk symbolizes a 2D-convolution. As the aperiodic filter ACFs are zero outside a $(2M-1)\times(2M-1)$-support, it is sufficient to extend the summation over a $(2M-1)\times(2M-1)$-window centred at (k, l). With (3) and (4), and taking into account the central symmetry $r_h^i(-m, -n) = r_h^i(m, n)$, the channel variance can be determined by

$$\sigma_i^2 = \sum_{m,n} r_s(m, n) \cdot r_h^i(m, n), \quad i = 1, \ldots, N. \tag{5}$$

As both $r_h^i(k, l)$ and $r_s(k, l)$ exhibit central symmetry, each one of the ACFs generally has no more than $2(N-M)+1$ different, independent coefficients inside the $(2M-1)\times(2M-1)$-window: the central element with $m = 0$, $n = 0$ occurs once, and all others twice. From the independent coefficients of $r_s(m, n)$ we form the $2(N-M)+1$-dimensional column vector r_s. Similarly, column vectors r_h^i are formed from the independent coefficients of $r_h^i(m, n)$, where each coefficient occurring twice is multiplied by a factor 2. Eq. (5) can now be written as the inner product

$$\sigma_i^2 = (r_h^i)^{\mathrm{T}} \cdot r_s. \tag{6}$$

Arranging the channel variances σ_i^2 into a column vector $p = (\sigma_1^2, \ldots, \sigma_N^2)^{\mathrm{T}}$, the following relation holds:

$$p = R_h \cdot r_s \quad \text{with } R_h = \begin{bmatrix} (r_h^1)^{\mathrm{T}} \\ \vdots \\ (r_h^N)^{\mathrm{T}} \end{bmatrix} \tag{7}$$

This linear mapping shows that the (estimated) channel variances characterize the portion of the ACF of the texture process inside a window of size $(2M-1)\times(2M-1)$. Textural properties which affect the ACF, such as directionality, coarseness, and periodicity, are thus reflected in these measures. Furthermore, as is already indicated by (5), each channel variance σ_i^2 measures the degree of similarity between the texture ACF and the corresponding filter ACF $r_h^i(k, l)$. However, the mapping is not injective, as the number of independent coefficients of each ACF exceeds the number N of filter masks. The matrix R_h thus is not a square one, but has the dimensions $(2(N-M)+1)\times N$, with $N = M^2$. Some information is lost during the transformation. This explains why the classification performance based on channel variances is slightly inferior to that of correlation methods, as reported in [23].

Let us now examine the computationally less demanding case of convolution by separable filter masks, where each filter response can be decomposed into two 1D-kernels $h_i^{\mathrm{hor}}(k)$ and $h_i^{\mathrm{ver}}(l)$, i.e. $h_i(k,l) = h_i^{\mathrm{hor}}(k)\cdot h_i^{\mathrm{ver}}(l)$, $i = 1, \dots, N$. The aperiodic ACFs of separable filters exhibit fourfold symmetry, i.e. $r_h^i(m,n) = r_h^i(-m,n) = r_h^i(m,-n) = r_h^i(-m,-n)$. This means that the number of independent coefficients of each ACF has reduced to N: the central coefficient $r_h^i(0,0)$ occurs once, the coefficients with either $m=0$ or $n=0$ occur twice, and all others four times. As described above, from the independent coefficients of each ACF $r_h^i(m,n)$ we form the N-dimensional column vector $\boldsymbol{r}_h^i$, where each coefficient is multiplied by the factor indicating how often it occurs (1, 2 or 4). For the special case of fourfold symmetrical texture ACFs,[2] the vector $\boldsymbol{r}_s$ can be reduced to N components, too. The mapping can now be written as done above (7), with the transformation matrix $\boldsymbol{R}_h$ being reduced to a quadratic one with dimensions $N \times N$, as the number of filters is identical to the number of independent coefficients of each ACF. The transformation is injective if filters with linearly independent aperiodic ACFs are chosen. The channel variances can then be regarded as coefficients of the vector $\boldsymbol{r}_s$ with respect to a basis formed by the column vectors of the matrix $(\boldsymbol{R}_h)^{-1}$. In this case, no information is lost in the course of the transformation. When regarding textures with fourfold symmetrical ACFs only, the filter bank approach should hence work as well as correlation methods for texture analysis.

3. Texture analysis by quadrature filter pairs

In this section, we link the discussed texture energy measures to an approach which extracts texture features by applying pairs of two-dimensional quadrature filters (e.g. [13]). For simplicity, we assume the random texture signals $s(x,y)$ to be defined over continuous spatial coordinates x, y. Information about the distribution of its power in different spectral bands can be obtained by applying a set of bandpass filters tuned to different orientations and spatial frequencies to $s(x,y)$, and computing the amplitude envelopes of the filter outputs.[3] Gaussian-shaped Gabor filters [9] are often used for this purpose as they minimize the uncertainty relation [7], thus optimizing the tradeoff between resolutions in the spatial and spectral domains [4, 5]. Such a filter has the complex impulse response

$$h(x,y) = h_{\mathrm{L}}(x,y)\exp\{\mathrm{j}2\pi(F_x x + F_y y)\}, \tag{8}$$

with $h_{\mathrm{L}}(x,y)$ real and Gaussian-shaped, and F_x and F_y being the centre frequencies of the bandpass. The real and imaginary components of this impulse response are (approximately) in quadrature. As the complex filter output $g(x,y) = s(x,y) * h(x,y)$ is a bandpass signal, it can be written as the product of a complex lowpass signal $g_{\mathrm{L}}(x,y)$ with a complex carrier, i.e.,

$$g(x,y) = g_{\mathrm{L}}(x,y)\exp\{\mathrm{j}2\pi(F_x x + F_y y)\}. \tag{9}$$

The amplitude envelope $|g_{\mathrm{L}}(x,y)|$ is a measure for the power of the texture signal contained in the passband of the filter. With the magnitudes of $g(x,y)$ and $g_{\mathrm{L}}(x,y)$ being identical, the amplitude envelope can be computed by $|g_{\mathrm{L}}(x,y)| = \sqrt{(\mathrm{Re}\{g(x,y)\})^2 + (\mathrm{Im}\{g(x,y)\})^2}$. The components $\mathrm{Re}\{g(x,y)\}$ and $\mathrm{Im}\{g(x,y)\}$ are available at the outputs of the quadrature filter pair formed from the real and imaginary part of $h(x,y)$.

Since the idea behind the quadrature filter method is to measure the power portions of the texture process contained in different spectral bands, the employed quadrature pairs are formed from narrowband filters, with their centre frequencies chosen such that the overlap between the transfer functions of different filter pairs is negligible.

[2] This holds for textures with rotation-invariant properties, or textures with directionalities parallel to the horizontal or vertical coordinate axes.

[3] The computational demand of carrying out the filtering for each one of possibly many orientations can be reduced considerably by using so-called steerable filter families, where filters sensitive to arbitrary orientations can be synthesized from a low number of basis filters by appropriate linear combination [8].

This means that the filter outputs are nearly uncorrelated, regardless of the correlations within $s(x, y)$.

As is well known from communication theory, an alternative to the quadrature filter approach for computing amplitude envelopes of bandpass-filtered signals is to subject the output of the (real) bandpass filter to a full-wave rectification, followed by a lowpass filtering operation [21, p. 154; 15]. This type of envelope detector receiver is commonly used for the demodulation of amplitude-modulated signals. In this case, the output signal $g(t)$ of the bandpass filter is the product of a real lowpass signal $f(t)$ with a real carrier $\cos(2\pi f_0 t)$, i.e. $g(t) = f(t)\cos(2\pi f_0 t)$. The spectrum of the rectified signal $|g(t)|$ consists of (weighted) spectra of the sought envelope $|f(t)|$ repeated with a period of $2f_0$ along the frequency axis. If the carrier frequency f_0 is higher than the cutoff frequency of the modulating lowpass signal $f(t)$, the zeroth spectrum can be recovered by an ideal-like lowpass, yielding an output signal $f_{\text{out}}(t)$ which is proportional to the amplitude envelope $|f(t)|$ of the bandpass signal $g(t)$ according to

$$f_{\text{out}}(t) = \frac{2}{\pi}|f(t)| \tag{10}$$

[21, p. 156].

3.1. Texture energy measures as envelope detectors

The demodulation procedure described above is resembled by one of the methods proposed by Laws in [14] for obtaining energy measures, namely that one which calculates the magnitude $|g_i(k, l)|$ inside each feature plane, followed by spatial averaging. Magnitude computation is identical to a full-wave rectification, and averaging is essentially a lowpass operation. This particular texture energy approach thus appears as an alternative to the computation of amplitude envelopes through quadrature filters. In contrast to the stated facts in communications, however, where the discussed approaches can be regarded as producing equivalent results, one can here expect the feature images resulting from magnitude computation and averaging only to approximate the amplitude envelopes obtained by means of quadrature filter pairs. The reason for this is that the spatial averaging filter used to recover the zeroth spectrum of $|g_L(k, l)|$ is not even approximately an ideal lowpass. The output of the texture energy chain thus corresponds to the sought ideal envelope $|g_L(k, l)|$ filtered by the non-ideal recovery lowpass. Note that replacing the averaging operation by an approximately ideal lowpass to mend this problem is not applicable in image processing, as this would lead to ringing artefacts at boundaries between different textures. As will be discussed later, however, other types of non-ideal lowpass filters are often better suited than a simple average to adapt the texture energy method to potential later processing steps like segmentation or edge detection.

3.2. Experimental comparisons

To illustrate how far the quadrature filter method and the texture energy approach can be regarded as similar under practical circumstances, textures were processed with the setup given in Fig. 1, where we have reverted to the discrete spatial coordinates (k, l): the texture signal $s(k, l)$ is filtered with a bandpass filter $h_R(k, l)$, which is the real part of the Gabor bandpass of Eq. (8), i.e. $h_R(k, l) = h_L(k, l)\cos(2\pi(F_x k + F_y l))$. From the thus filtered texture, a signal $g_1(k, l)$ is computed by rectification and subsequent lowpass filtering. The

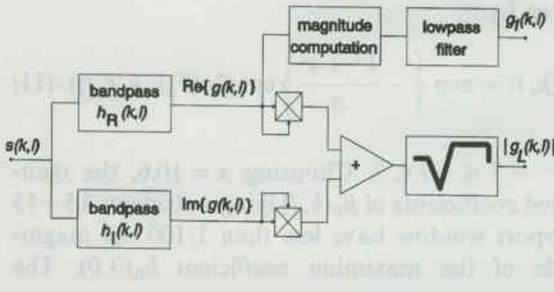

Fig. 1. Block diagram of the setup to compare the approaches discussed in the text. The signal $g_1(k, l)$ is a lowpass approximation to the amplitude envelope of the bandpass-filtered texture, whereas $|g_L(k, l)|$ is the amplitude envelope computed using the quadrature filter pair $h_R(k, l) = h_L(k, l)\cos(2\pi(F_x k + F_y l))$ and $h_I(k, l) = h_L(k, l)\sin(2\pi(F_x k + F_y l))$.

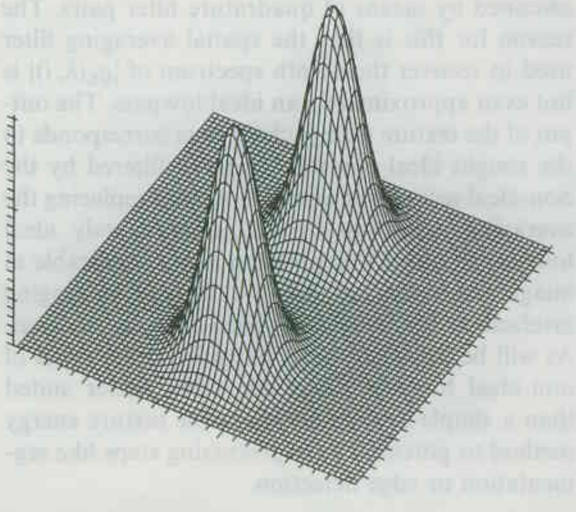

Fig. 2. Frequency response of the bandpass filter kernel $h_R(k, l) = \exp\{-(k^2 + l^2)/10.6\}\cos(2\pi \cdot l/4)$ (kernel restricted to a 15×15 support window).

only difference to the texture energy approach of [14] is that we have replaced the averaging operation by the Gaussian lowpass filter $h_L(k, l)$. Additionally, the envelope $|g_L(k, l)|$ of the bandpass-filtered texture is computed as described at the beginning of this section. The filter $h_I(k, l)$ in the lower branch of Fig. 1 is the imaginary part of $h(k, l)$, i.e. $h_I(k, l) = h_L(k, l)\sin(2\pi(F_x k + F_y l))$. The filtering operations were implemented as convolutions in the spatial domain, with the bandpass filter masks defined on a support area of 15×15 pixels.[4] A filter example is given in Fig. 2. Its impulse response is given by

$$h_R(k, l) = \exp\left\{-\frac{k^2 + l^2}{\alpha}\right\}\cos(2\pi(F_x k + F_y l)) \quad (11)$$

for $-7 \leqslant k, l \leqslant 7$. Choosing $\alpha = 10.6$, the truncated coefficients of $h_R(k, l)$ lying outside its 15×15 support window have less than 1/100 the magnitude of the maximum coefficient $h_R(0,0)$. The centre frequency of the bandpass was chosen to $(F_x, F_y) = (0, 0.25)$.[5]

[4] Details of the filter design are beyond the scope of this contribution, as is segmentation. Ample proposals for both can be found in the references.

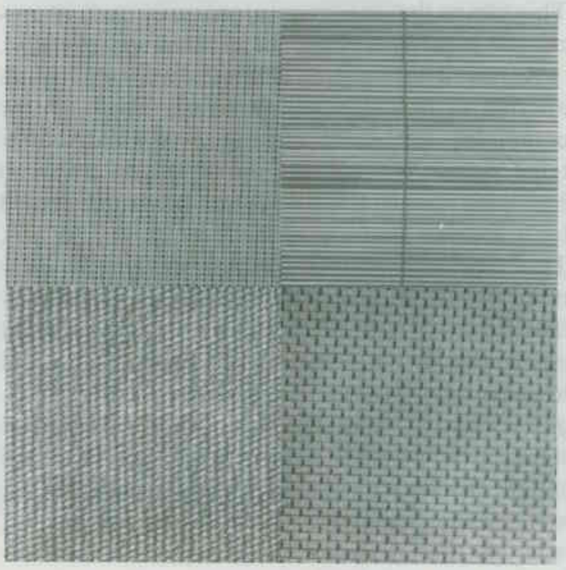

Fig. 3. Original textured image.

Fig. 4 shows the resulting feature images for the textured picture of Fig. 3. The similarity of the results $g_1(k, l)$ obtained by rectifying and lowpass filtering to the amplitude envelopes $|g_L(k, l)|$ acquired by the quadrature filter pair is evident. However, the amplitude envelopes follow sudden changes, like sharp 'dropouts' in the original textures or transitions between areas with different textures much better than their counterparts resulting from the texture energy approach, which are distorted by the non-ideal recovery lowpass.

According to what was said in Section 3.1, the differences between the feature images obtained by quadrature filters and those acquired by the texture energy method should vanish once the former are also subjected to the same lowpass filter $h_L(k, l)$ which is employed by the texture energy method. Fig. 5, where the result from the right-hand side of Fig. 4 has been convolved with $h_L(k, l)$, shows that this is indeed the case.

[5] These frequency notations are normalized with the image size. For a picture of 256×256 pixels, $F_y = 0.25$ corresponds to 64 cycles/image.

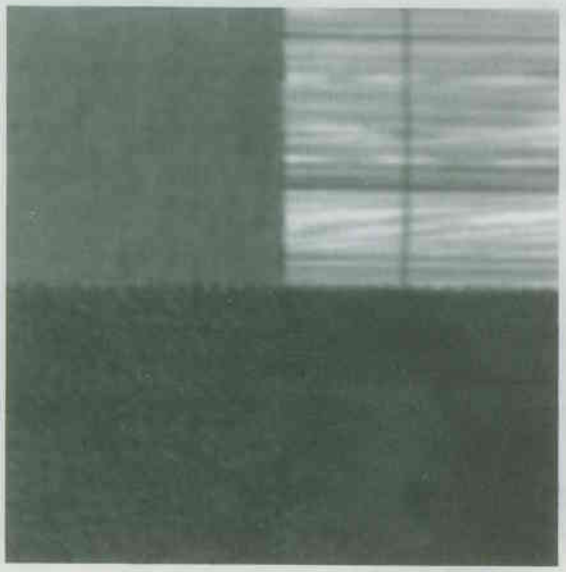

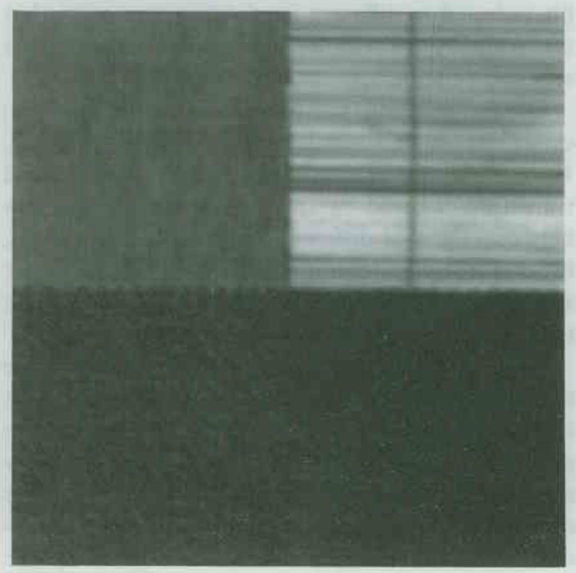

Fig. 4. Feature images computed from Fig. 3, using the filter mask corresponding to Fig. 2. Left: result obtained by computation of magnitude and lowpass filtering. Right: amplitude envelope produced by the quadrature filter pair $h_R(k, l)$ and $h_I(k, l)$. Both pictures have been scaled to fit the interval [0, 255].

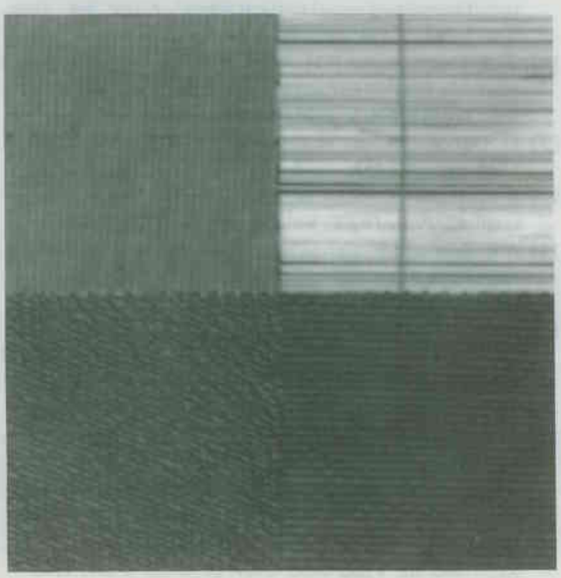

Fig. 5. Lowpass-filtered versions of the amplitude envelopes depicted on the right-hand side of Fig. 4. The lowpass used was the separable lowpass equivalent $h_L(k, l)$ of the bandpass filter $h_R(k, l)$, i.e. $h_L(k, l) = \exp\{-(k^2 + l^2)/10.6\}$, restricted to a 15×15 support window.

4. Conclusions and summary

In connection with further processing of texture features, the consequences of the above facts are the following. Certain types of further processing of texture features – e.g. by segmentation as in [13; 4, Chapter 5B], or by edge detection [16, 22] – often require that the features are first lowpass filtered. As lowpass filtering the quadrature filter features produces results nearly identical to texture energy features, the computationally cheaper texture energy method would in such cases be sufficient. The type of processing intended, however, has implications for the design of the texture energy lowpass used, which now serves the double function of recovering the zeroth-order feature spectrum *and* preparing the features for the following processing stage: in edge detection, for instance, Gaussian-like-shaped filter kernels should be chosen. Rectangularly shaped filters, like the ones originally used in the texture energy method, are well known to perform inadequately [22, pp. 150, 160]. The bandpass filters employed by the texture energy method may consist of even-symmetric Gabor filters tuned to different spatial frequencies, so that the validity of established filter bank design schemes remains untouched.

On the other hand, pixel-based (multispectral) classification and segmentation schemes like [12, 19, 1, 17] may be adversely affected by smeared transitions caused by the texture energy lowpass between areas of different textures. In these cases, the quadrature filter approach would thus be better suited than the texture energy method to provide the texture features.

In summary, this contribution first discussed the relationship between texture energy measures at the output of a filter bank applied to texture signals and the ACF of the texture process. For stationary signals, the relationship was shown to be a linear one, which is not generally injective. The coefficients of the transform matrix were given by the coefficients of the aperiodic autocorrelation functions of the filter impulse responses.

Drawing analogies to communication theory, we then showed that the texture energy method can be traced back to the same concept of demodulating envelopes from which also the quadrature filter approach to texture analysis evolved. Replacing the mostly small filter masks preferably used in the texture energy method by truncated Gabor bandpass filters, the similarity between the results produced by both methods could be demonstrated. A comparison showed the superior ability of the quadrature filter pair approach to reconstruct high-frequency components in the envelope images. Criteria for choosing the approach better suited to texture analysis with respect to the intended further processing steps as well as points which should be considered when designing the lowpass filter in the texture energy method were discussed.

Finally, let us note that the texture energy approach does not yield the phase envelope of the bandpass filtered signal, which can be obtained from the complex filter output $g(x, y)$ in (9). Variations in the phase envelope have been used to discriminate between shifted versions of otherwise identical texture, e.g. by locating zero crossings in the Laplacian of the phase envelope (cf. [5, Chapter 4]). Such discrimination would not be possible by the texture energy approach.

References

[1] T. Aach, U. Franke and R. Mester, "Top-down image segmentation using object detection and contour relaxation", *Proc. Internat. Conf. Acoust. Speech Signal Process. 89*, Glasgow, UK, May 1989, pp. 1703–1706.

[2] T. Aach, R. Mester and U. Franke, "From texture energy measures to quadrature filter pairs – A system theoretical view of texture feature extraction", in: J.L. Lacoume et al., eds., *Proc. EUSIPCO 88*, *Signal Processing IV: Theories and Applications*, Grenoble, France, September 1988, pp. 827–830.

[3] F. Ade, "Characterization of textures by 'eigenfilters'", *Signal Processing*, Vol. 5, No. 5, September 1983, pp. 451–457.

[4] A.C. Bovik, "Analysis of multichannel narrow-band filters for image texture segmentation", *IEEE Trans. Signal Process.*, Vol. 39, No. 9, 1991, pp. 2025–2043.

[5] A.C. Bovik, M. Clark and W.S. Geisler, "Multichannel texture analysis using localized spatial filters", *IEEE Trans. Pattern Anal. Machine Intell.*, Vol. 12, No. 1, 1990, pp. 55–73.

[6] P. Cohen, C.T. LeDinh and V. Lacasse, "Classification of natural textures by means of two-dimensional orthogonal masks", *IEEE Trans. Acoust. Speech Signal Process.*, Vol. 37, No. 1, 1989, pp. 125–128.

[7] J.G. Daugman, "Uncertainty relation for resolution in space, spatial frequency, and orientation optimized by two-dimensional visual cortical filters", *J. Opt. Soc. Amer.*, Vol. 2, No. 7, 1985, pp. 1160–1169.

[8] W.T. Freeman and E.H. Adelson, "The design and use of steerable filters", *IEEE Trans. Pattern Anal. Machine Intell.*, Vol. 13, No. 9, 1991, pp. 891–906.

[9] D. Gabor, "Theory of communication", *J. IEE*, Vol. 93, 1946, pp. 429–457.

[10] R.M. Haralick, "Statistical and structural approaches to texture", *Proc. IEEE*, Vol. 67, 1979, pp. 786–804.

[11] A.K. Jain and F. Farrokhnia, "Unsupervised texture segmentation using Gabor filters", *Pattern Recognition*, Vol. 24, No. 12, 1991, pp. 1167–1186.

[12] R.L. Kettig and D.A. Landgrebe, "Classification of multispectral image data by extraction and classification of homogeneous objects", *IEEE Trans. Geosci. Electr.*, Vol. 14, No. 1, 1976, pp. 19–26.

[13] H. Knutsson and G.H. Granlund, "Texture analysis using two-dimensional quadrature filters", *IEEE Works. Comp. Archit. Pattern Anal. Image Data Base Manag.*, Pasadena, California, October 1983.

[14] K.I. Laws, Textured image segmentation, Ph.D. Thesis, Rept. 940, Im. Proc. Inst., Univ. of South. Calif., 1980.

[15] H.D. Lüke, *Signalübertragung*, Springer, Berlin, 1992.

[16] D. Marr and E. Hildreth, "Theory of edge detection", *Proc. Roy. Soc. London B*, Vol. 207, 1980, pp. 187–217.

[17] R. Mester, T. Aach and U. Franke, "Image segmentation experiments using the contour relaxation algorithm", *Zeitschr. Photogramm. Fernerkund.*, Vol. 4, July 1991, pp. 127–132.

[18] A.V. Oppenheim and R.W. Schafer, *Digital Signal Processing*, Prentice-Hall, Englewood Cliffs, NJ, 1975.

[19] S. Peleg, "A new probabilistic relaxation scheme", *IEEE Trans. Pattern Anal. Machine Intell.*, Vol. 2, 1980, pp. 362–369.

[20] M. Pietikaïnen, A. Rosenfeld and L.S. Davis, "Experiments with texture classification using averages of local pattern matches", *IEEE Trans. System Man Cybernet.*, Vol. 13, No. 3, 1983, pp. 421–426.

[21] D.J. Sakrison, *Communication Theory*, Wiley, New York, 1968.

[22] V. Torre and T. Poggio, "On edge detection", *IEEE Trans. Pattern Anal. Machine Intell.*, Vol. 8, No. 2, 1986, pp. 147–163.

[23] M. Unser, "Local linear transforms for texture measurements", *Signal Processing*, Vol. 11, No. 1, July 1986, pp. 61–79.

[24] M. Unser and M. Eden, "Multiresolution feature extraction and selection for texture segmentation", *IEEE Trans. Pattern Anal. Machine Intell.*, Vol. 11, No. 7, 1989, pp. 717–728.

[25] M. Unser and M. Eden, "Nonlinear operators for improving texture segmentation based on features extracted by spatial filtering", *IEEE Trans. System Man Cybernet.*, Vol. 20, No. 4, 1990, pp. 804–815.

[26] L. van Gool, P. Dewaele and A. Oosterlinck, "Texture analysis anno 1983", *Comput. Vision Graph. Image Process.*, Vol. 29, 1985, pp. 336–357.